https://doi.org/10.2352/ISSN.2169-2629.2017.32.59

Spectral Image Analysis of Florescent Objects with Mutual Illumination

Shoji Tominaga, Keiji Kato, Keita Hirai, and Takahiko Horiuchi
Graduate School of Advanced Integration Science, Chiba University, Chiba, Japan

Abstract

This paper proposes a method to analyze the observed images of fluorescent images influenced by mutual illumination and estimate the spectral components. We suppose a general case where the entire surfaces of fluorescent objects have mutual illumination effects. First we model mutual illumination between the two objects. It is shown that the spectral composition is summarized with four components of (1) diffuse reflection, (2) diffuse-diffuse interreflection, (3) fluorescent self-luminescence, and (4) interreflection by mutual fluorescent illumination. Each component has two unknown factors of the spectral functions depending on wavelength and the weighting factors depending on pixel location. Second, an iterative algorithm is developed to solve this nonlinear estimation problem. Moreover, aiming a general solution which is independent of the initial conditions, we adopt a stabilization index to enforce the spectral smoothness and the spatial smoothness. Finally, the feasibility of the proposed method is shown using the spectral images of two adjacent fluorescent objects captured by a spectral imaging system in the visible range.

Introduction

When multiple objects are located closely, the phenomenon called interreflection or mutual illumination is observed on the object surfaces. In such a case, the illumination consists of at least two distinct parts: the direct illumination from a primary light source, and the indirect or mutual illumination, created by light coming from the other object surfaces. The mutual illumination is accompanied with a change in the appearance of the object surfaces. The problems of mutual illumination analysis were studied in a variety of field such as color science, imaging technology, computer vision, and computer graphics [1]-[8]. However, in most of the previous studies, non-fluorescent objects such as matte object and inhomogeneous dielectric object were used.

When two or more fluorescent objects are located closely, an object surface is illuminated by fluorescence emitted from the nearby object surfaces as an indirect illumination, which causes light reflection and fluorescence excitation on the target object. We note that the mutual illumination phenomenon between the fluorescent objects is composed by two types of mutual illumination on the basis of light reflection and fluorescence emission. In our previous study [9], we proposed a method to estimate the spectral image components from the captured images of two closely apposed fluorescent objects. We supposed that we knew the exact Donaldson matrices, representing the bispectral characteristics of the fluorescent objects. Then the problem of component estimation was reduced to a linear estimation problem. As a result, the observed image was decomposed into several spectral component images. However, it should be noted that, if the object surfaces are influenced by mutual illumination, we cannot have exact knowledge about the bispectral characteristics of the fluorescent objects.

The present paper supposes a general case where the entire surfaces of fluorescent objects have mutual illumination effects. We develop a method to analyze the observed images influenced by the mutual illumination and estimate the spectral components. First, we model mutual illumination between the two objects. We show that the observed spectral images are described by a system of nonlinear equations which have two factors: one factor is spectral functions depending on wavelength and another is the weighting factors depending on pixel location. Concerning the former factor, we have various spectral functions composed of two surface reflectances and two fluorescent emissions. Therefore, we have to solve a multiplication of two types of unknown factors: the bispectral functions and the location weighting coefficients. The model is more precise and generalized than our recent model [10]. Second, we propose an iterative algorithm to estimate the spectral functions and the location weights. Moreover, aiming a general solution which is independent of the initial conditions, we adopt a stabilization index to enforce the spectral smoothness and the spatial smoothness. In this experiments, the spectral images are captured using a spectral imaging system in the visible range (400, 700 nm) under an incandescent lamp and a sunlight lump. Finally, the feasibility of the proposed method is shown in the case of mutual illumination.

Model of Two Fluorescent Objects with Mutual Illumination

A Donaldson matrix $D(\lambda_{em},\lambda_{ex})$ represents the bispectral radiance factor of a fluorescent object as a two-variable function of the excitation wavelength λ_{ex} and the emission/reflection wavelength λ_{em}. The diagonal of $D(\lambda_{em},\lambda_{ex})$ represents the surface-spectral reflectance $S(\lambda)$, and the lower half of the off-diagonal represents the luminescent component by fluorescent emission. The luminescent radiance factor is separated into the emission and excitation wavelength components as $D_L(\lambda_{em},\lambda_{ex}) = \alpha(\lambda_{em})\beta(\lambda_{ex})$. A discrete form of the Donaldson matrix can be represented in an $N \times N$ matrix as

$$\mathbf{D} = \mathbf{D}_{\text{ref}} + \mathbf{D}_{\text{lum}} = \begin{bmatrix} s_1 & 0 & \cdots & 0 \\ 0 & s_2 & \ddots & \vdots \\ \vdots & \ddots & \ddots & 0 \\ 0 & \cdots & 0 & s_N \end{bmatrix} + \begin{bmatrix} 0 & & \cdots & & 0 \\ \alpha_2\beta_1 & 0 & & & \\ \alpha_3\beta_1 & \alpha_3\beta_2 & 0 & & \vdots \\ \vdots & \vdots & \ddots & \ddots & \\ \alpha_N\beta_1 & \alpha_N\beta_2 & \cdots & \alpha_N\beta_{N-1} & 0 \end{bmatrix} \quad (1)$$

where $\mathbf{D}_{\text{ref}}$ is a diagonal matrix with elements (i = 2, 3, .., N) representing the reflected radiance factor, and $\mathbf{D}_{\text{lum}}$ is a triangular

matrix of the luminescent radiance factor with elements α_i (i = 2, 3, .., N), and β_i (i = 1, 2, .., N - 1) representing the emission spectrum and the excitation spectrum, respectively [11],[12]. The norm of the excitation spectral vector $\boldsymbol{\beta}$ is normalized as $\|\boldsymbol{\beta}\| = 1$.

Let us suppose two fluorescent objects with matte surfaces are located closely as shown in Figure 1, where a mutual illumination occurs between the two surfaces with different Donaldson matrices. The two surfaces are illuminated uniformly with a single light source. The spectral compositions observed on Surfaces 1 and 2 are decomposed into two components of the direct illumination from the light source and the mutual illumination between the two surfaces, which are described as the following forms:

$$\begin{aligned}&\text{Surface 1:}\ \left\{\left(\mathbf{D}_{R1}+\mathbf{D}_{L1}\right)+\left(\mathbf{D}_{R1}+\mathbf{D}_{L1}\right)\left(\mathbf{D}_{R2}+\mathbf{D}_{L2}\right)\right\}\mathbf{e}\\&\text{Surface 2:}\ \left\{\left(\mathbf{D}_{R2}+\mathbf{D}_{L2}\right)+\left(\mathbf{D}_{R2}+\mathbf{D}_{L2}\right)\left(\mathbf{D}_{R1}+\mathbf{D}_{L1}\right)\right\}\mathbf{e}\end{aligned} \tag{2}$$

where $\mathbf{e}$ denotes an N-dimensional illuminant vector of a discrete representation of $E(\lambda)$.

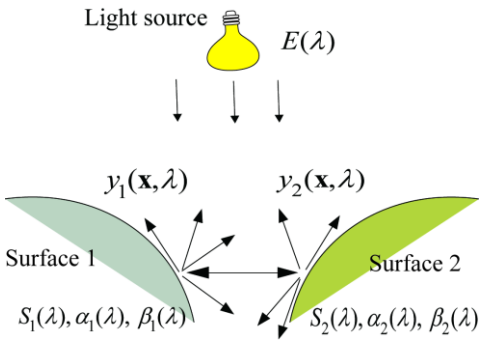

Figure 1. Two object surfaces with different bispectral characteristics under a uniform illumination.

On the basis of the above properties of spectral composition, we describe the spectral model of mutual illumination by the continuous functions of wavelength as shown in Eq.(3). The observations of spectral radiances at location $\mathbf{x}$ of Surface 1 and Surface 2 are represented as

$$\begin{aligned}y_1(\mathbf{x},\lambda_{em}) &= f_{11}(\mathbf{x})S_1(\lambda_{em})E(\lambda_{em}) + f_{12}(\mathbf{x})S_1(\lambda_{em})S_2(\lambda_{em})E(\lambda_{em})\\&+ f_{13}(\mathbf{x})\alpha_1(\lambda_{em})\int\beta_1(\lambda_{ex})E(\lambda_{ex})d\lambda_{ex}\\&+ f_{14}(\mathbf{x})\alpha_1(\lambda_{em})\int\beta_1(\lambda_{ex})S_2(\lambda_{ex})E(\lambda_{ex})d\lambda_{ex}\\&+ f_{15}(\mathbf{x})\alpha_1(\lambda_{em})\int\beta_1(\lambda_{ex})\alpha_2(\lambda_{ex})\left(\int\beta_2(\lambda_{ex}')E(\lambda_{ex}')d\lambda_{ex}'\right)d\lambda_{ex}\\&+ f_{16}(\mathbf{x})S_1(\lambda_{em})\alpha_2(\lambda_{em})\int\beta_2(\lambda_{ex})E(\lambda_{ex})d\lambda_{ex}\\y_2(\mathbf{x},\lambda_{em}) &= f_{21}(\mathbf{x})S_2(\lambda_{em})E(\lambda_{em}) + f_{22}(\mathbf{x})S_1(\lambda_{em})S_2(\lambda_{em})E(\lambda_{em})\\&+ f_{23}(\mathbf{x})\alpha_2(\lambda_{em})\int\beta_2(\lambda_{ex})E(\lambda_{ex})d\lambda_{ex}\\&+ f_{24}(\mathbf{x})\alpha_2(\lambda_{em})\int\beta_2(\lambda_{ex})S_1(\lambda_{ex})E(\lambda_{ex})d\lambda_{ex}\\&+ f_{25}(\mathbf{x})\alpha_2(\lambda_{em})\int\beta_2(\lambda_{ex})\alpha_1(\lambda_{ex})\left(\int\beta_1(\lambda_{ex}')E(\lambda_{ex}')d\lambda_{ex}'\right)d\lambda_{ex}\\&+ f_{26}(\mathbf{x})S_2(\lambda_{em})\alpha_1(\lambda_{em})\int\beta_1(\lambda_{ex})E(\lambda_{ex})d\lambda_{ex}\end{aligned} \tag{3}$$

where the interval of integration is [350, λ_{em}], all weights $f_{ij}(\mathbf{x})$ are variable of location $\mathbf{x}$ and independent of wavelength λ. It should be noted that all integrations in Eq.(3) produce constant values. When we summarize the different terms with the same spectral composition into one group, the above observation equations are simplified and grouped based on the spectral components as in the form:

$$\begin{aligned}y_1(\mathbf{x},\lambda_{em}) &= F_{11}(\mathbf{x})S_1(\lambda_{em})E(\lambda_{em}) + F_{12}(\mathbf{x})S_1(\lambda_{em})S_2(\lambda_{em})E(\lambda_{em})\\&+ C_{11}(\lambda_{em})F_{13}(\mathbf{x})\alpha_1(\lambda_{em}) + C_{12}(\lambda_{em})F_{14}(\mathbf{x})S_1(\lambda_{em})\alpha_2(\lambda_{em})\\y_2(\mathbf{x},\lambda_{em}) &= F_{21}(\mathbf{x})S_2(\lambda_{em})E(\lambda_{em}) + F_{22}(\mathbf{x})S_1(\lambda_{em})S_2(\lambda_{em})E(\lambda_{em})\\&+ C_{21}(\lambda_{em})F_{23}(\mathbf{x})\alpha_2(\lambda_{em}) + C_{22}(\lambda_{em})F_{24}(\mathbf{x})S_2(\lambda_{em})\alpha_1(\lambda_{em})\end{aligned} \tag{4}$$

where $C_{11}, C_{12}, C_{21}, C_{22}$ are not constant, differently from [10], which are calculated from the spectra of excitation, reflection, and illuminant. Note that the observed radiance factors consist of only four spectral components $S_1(\lambda)E(\lambda)$ ($S_2(\lambda)E(\lambda)$), $S_1(\lambda)S_2(\lambda)E(\lambda)$ ($S_2(\lambda)S_1(\lambda)E(\lambda)$), $\alpha_1(\lambda)$ ($\alpha_2(\lambda)$), and $S_1(\lambda)\alpha_2(\lambda)$ ($S_2(\lambda)\alpha_1(\lambda)$). These components correspond to (1) diffuse reflection, (2) diffuse-diffuse interreflection, (3) fluorescent self-luminescence, and (4) interreflection caused by the fluorescent illumination from the adjacent surface.

We can summarize the observation model in a matrix form. Let $\mathbf{s}_1(\mathbf{s}_2)$ and $\boldsymbol{\alpha}_1(\boldsymbol{\alpha}_2)$ be N-dimensional column vectors representing the reflectance and emission spectra. Also, let $\mathbf{F}_1(\mathbf{x})(\mathbf{F}_2(\mathbf{x}))$ be 4-dimensional column vectors representing the location weights and $\mathbf{A}_1(\mathbf{A}_2)$ be an $N \times 4$ matrices as follows:

$$\begin{aligned}\mathbf{A}_1 &= \left[\mathbf{s}_1\circ\mathbf{e}\quad \mathbf{s}_1\circ\mathbf{s}_2\circ\mathbf{e}\quad \mathbf{c}_{11}\circ\boldsymbol{\alpha}_1\quad \mathbf{c}_{12}\circ\mathbf{s}_1\circ\boldsymbol{\alpha}_2\right],\\\mathbf{A}_2 &= \left[\mathbf{s}_2\circ\mathbf{e}\quad \mathbf{s}_1\circ\mathbf{s}_2\circ\mathbf{e}\quad \mathbf{c}_{21}\circ\boldsymbol{\alpha}_2\quad \mathbf{c}_{22}\circ\mathbf{s}_2\circ\boldsymbol{\alpha}_1\right]\\\mathbf{F}_1(\mathbf{x}) &= \left[F_{11}(\mathbf{x})\quad F_{12}(\mathbf{x})\quad F_{13}(\mathbf{x})\quad F_{14}(\mathbf{x})\right]^t,\\\mathbf{F}_2(\mathbf{x}) &= \left[F_{21}(\mathbf{x})\quad F_{22}(\mathbf{x})\quad F_{23}(\mathbf{x})\quad F_{24}(\mathbf{x})\right]^t\end{aligned} \tag{5}$$

where symbols $\circ$ and t represent element-wise multiplication and matrix transposition, respectively. Then the observations with mutual illumination effects are modeled in a simple matrix equation as

$$\begin{aligned}\mathbf{y}_1(\mathbf{x}) &= \mathbf{A}_1\mathbf{F}_1(\mathbf{x}),\\\mathbf{y}_2(\mathbf{x}) &= \mathbf{A}_2\mathbf{F}_2(\mathbf{x}).\end{aligned} \tag{6}$$

Estimation Method of Spectral Image Components

Iterative estimation algorithm

Figure 2 shows the surface observations in the joint range of wavelength λ and location $\mathbf{x}$. If both surfaces are influenced by mutual illumination, we cannot obtain the exact Donaldson matrices. In such a case, we have to estimate the spectral functions and the location weights from the observations. This estimation leads to a nonlinear estimation problem to minimize a residual error $\|\mathbf{y} - \mathbf{AF}\|^2$, where both $\mathbf{A}$ and $\mathbf{F}$ are unknown. In this paper, we propose an iterative approach to solve this nonlinear estimation problem. We note that the wavelength range of fluorescent

emission $\alpha(\lambda)$ can be measured by using a separate way such as the use of a UV light source. Moreover, we suppose a weak influence of interreflection where the effect is canceled out between two opponent color surfaces. In such a case we can predict the possible spectral functions of each surface. Under this situation, the unknown quantities to be estimated are the relative shapes of spectral functions $S(\lambda)$, $\alpha(\lambda)$, $\beta(\lambda)$ and the location weights $F_1(\mathbf{x}), F_2(\mathbf{x}), F_3(\mathbf{x}), F_4(\mathbf{x})$ for each object surface.

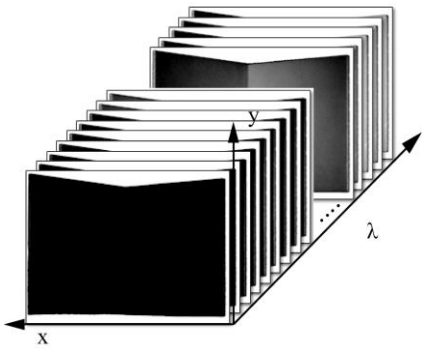

Figure 2. Surface observations in the joint range of wavelength λ and location x=(x,y).

Our iterative approach is based on an alternate estimation of the spectral functions and the location weights. Instead of the joint minimization over variables λ and $\mathbf{x}$, we separate the minimization into two steps of a linear least squares estimation. The observation functions with two variables λ and $\mathbf{x}$ are expressed in two equivalent forms as follows:

$$y_1(\mathbf{x},\lambda) = \begin{bmatrix} S_1(\lambda)E(\lambda) & S_1(\lambda)S_2(\lambda)E(\lambda) & C_{11}\alpha_1(\lambda) & C_{12}S_1(\lambda)\alpha_2(\lambda) \end{bmatrix} \begin{bmatrix} F_{11}(\mathbf{x}) \\ F_{12}(\mathbf{x}) \\ F_{13}(\mathbf{x}) \\ F_{14}(\mathbf{x}) \end{bmatrix}$$

$$y_2(\mathbf{x},\lambda) = \begin{bmatrix} S_2(\lambda)E(\lambda) & S_1(\lambda)S_2(\lambda)E(\lambda) & C_{21}\alpha_2(\lambda) & C_{22}S_2(\lambda)\alpha_1(\lambda) \end{bmatrix} \begin{bmatrix} F_{21}(\mathbf{x}) \\ F_{22}(\mathbf{x}) \\ F_{23}(\mathbf{x}) \\ F_{24}(\mathbf{x}) \end{bmatrix} \quad (7)$$

and

$$\begin{bmatrix} y_1(\mathbf{x},\lambda) \\ y_2(\mathbf{x},\lambda) \end{bmatrix} = \begin{bmatrix} F_{11}(\mathbf{x})E(\lambda) & 0 & F_{12}(\mathbf{x})E(\lambda) & C_{11}(\lambda)F_{13}(\mathbf{x}) & 0 & C_{12}(\lambda)F_{14}(\mathbf{x}) & 0 \\ 0 & F_{21}(\mathbf{x})E(\lambda) & F_{22}(\mathbf{x})E(\lambda) & 0 & C_{21}(\lambda)F_{23}(\mathbf{x}) & 0 & C_{22}(\lambda)F_{24}(\mathbf{x}) \end{bmatrix} \begin{bmatrix} S_1(\lambda) \\ S_2(\lambda) \\ S_1(\lambda)S_2(\lambda) \\ \alpha_1(\lambda) \\ \alpha_2(\lambda) \\ S_1(\lambda)\alpha_2(\lambda) \\ S_2(\lambda)\alpha_1(\lambda) \end{bmatrix} \quad (8)$$

Eq. (7) is used for determining the location weights by the linear least squares method when the spectral functions are fixed. Also Eq. (8) is used for determining the spectral functions when the location weights are fixed. Therefore, minimization of the residual error is performed by estimating the spectral functions and the location weights alternately, based on the linear least square minimization with non-negativity constraints. All estimates are updated in two steps. We repeat this iterative process with appropriate initial conditions of the spectral functions. In Eq.(8) the spectral functions include the spectral multiplication terms $S_1(\lambda)S_2(\lambda)$, $S_1(\lambda)\alpha_2(\lambda)$, and $S_2(\lambda)\alpha_1(\lambda)$. Although these terms are estimated by the least squares method as independent variables, the estimates are not related to the estimates of $S_1(\lambda)$, $S_2(\lambda)$, $\alpha_1(\lambda)$, and $\alpha_2(\lambda)$. In the range where there is no fluorescent emission of $\alpha(\lambda) = 0$, a simplified matrix equation is used for updating the remaining spectral functions.

In a practical iterative estimation algorithm, the vector length of each spectral function is known in advance, that is, the L2-norms $\|\mathbf{s}_1\|$, $\|\mathbf{s}_2\|$, $\|\boldsymbol{\alpha}_1\|$, $\|\boldsymbol{\alpha}_2\|$, $\|\boldsymbol{\beta}_1\|(=1)$, $\|\boldsymbol{\beta}_2\|(=1)$ are given as a priori knowledge. The initial conditions in the iterative estimation $\beta(\lambda)$ of spectral functions are set to constant spectra with the given norms. The excitation spectral function of each surface is estimated in a separate way without using the iterative algorithm. When the spectral reflectance estimation of $S(\lambda)$ is updated at each step of the iterative process, the excitation spectrum can be estimated by substituting the reflectance estimate $\hat{S}(\lambda)$ into the following relationship:

$$\beta(\lambda) = Q(\lambda)\left(1 - \hat{S}(\lambda)\right) \quad (9)$$

where $Q(\lambda)$ is the luminescence efficiency [11].

It is shown in the later experiments that the proposed iterative algorithm converges rapidly.

Norm estimation of spectral functions

If the surface is influenced by strong interreflection, the apparent spectral function, especially surface reflectance, is usually larger than the original reflectance without interreflection. As a result the norms of the spectral functions are likely increased. In this section, we consider how to estimate the norms in order to further generalize the algorithm. Let K be a scale factor to transform the previously given reflectance norm $\|\mathbf{s}\|$ to true norm in the form $K \times \|\mathbf{s}\|$. Note that the observations are multiplications of the spectral functions and the location weights. Therefore, if the scale factor is estimated as K_1, the spectral reflectance estimate $\hat{S}(\lambda)$ and the location weight are corrected into $K_1 \times \hat{S}(\lambda)$ and $1/K_1 \times \hat{F}(\mathbf{x})$, respectively. Also the spectral luminescence $\hat{\alpha}(\lambda)$ and its location weight $\hat{F}(\mathbf{x})$ are corrected in the same way as $K_2 \times \hat{\alpha}(\lambda)$ and $1/K_2 \times \hat{F}(\mathbf{x})$. Therefore our task is to determine the

scale parameter K based on the obtained set of estimates.

Smoothness constraint is introduced as an evaluation index for K. We have two smoothness constraints on the spectral functions and the surface location weights. The roughness (smoothness) of the spectral functions is calculated from difference data between adjacent wavelengths $(\lambda_i, \lambda_{i+1})$ in the equations $\sum_\lambda \hat{s}_\lambda^2$ and $\sum_\lambda \hat{\alpha}_\lambda^2$, where the wavelength ranges are [400, 700nm] for spectral reflectance and the emission range for spectral luminescence in this paper. The roughness of the location weights is calculated from two-dimensional difference data between the adjacent pixels (x_i, x_{i+1}) and (y_i, y_{i+1}) in the equation $\left(\sum_x \hat{F}_x^2 + \sum_y \hat{F}_y^2\right)$, where the location range is a two-dimensional area specified by the observed image. Because the two types of roughness are in different dimensions, we may consider a parameter to balance the two roughnesses for determining K. Let ρ be a balancing parameter.

Based on the above preparations, the evaluation index of smoothness constraint is described as follows:

$$E = E_1 + E_2 + E_3 + E_4 = \left(K_1^2 A_1 + \frac{\rho_1}{K_1^2} B_1\right) + \left(K_2^2 A_2 + \frac{\rho_2}{K_2^2} B_2\right) + \left(K_3^2 A_3 + \frac{\rho_3}{K_3^2} B_3\right) + \left(K_4^2 A_4 + \frac{\rho_4}{K_4^2} B_4\right) \quad (10)$$

where

$$A_1 = \frac{1}{W_1}\sum_\lambda \hat{s}_{1\lambda}^2,\ A_2 = \frac{1}{W_2}\sum_\lambda \hat{s}_{2\lambda}^2,\ A_3 = \frac{1}{W_3}\sum_\lambda \hat{\alpha}_{1\lambda}^2,\ A_4 = \frac{1}{W_4}\sum_\lambda \hat{\alpha}_{2\lambda}^2$$
$$B_1 = \frac{1}{R_1}\left(\sum_x \hat{F}_{11x}^2 + \sum_y \hat{F}_{11y}^2\right),\ B_2 = \frac{1}{R_2}\left(\sum_x \hat{F}_{21x}^2 + \sum_y \hat{F}_{21y}^2\right),$$
$$B_3 = \frac{1}{R_3}\left(\sum_x \hat{F}_{13x}^2 + \sum_y \hat{F}_{13y}^2\right),\ B_4 = \frac{1}{R_4}\left(\sum_x \hat{F}_{23x}^2 + \sum_y \hat{F}_{23y}^2\right) \quad (11)$$

In Eq.(11) W_i and R_i $(i = 1, 2, ..., 4)$ represent the wavelength ranges and the image size, respectively. The optimal scale factors are then obtained by minimizing each term of the smoothness index E individually as

$$K_i = \sqrt[4]{\frac{\rho_i B_i}{A_i}},\quad (i = 1, 2, ..., 4) \quad (12)$$

Finally, the balancing parameters ρ_i (i = 1, 2,…, 4) are chosen empirically based on the experiments because these cannot be determined analytically nor theoretically. In this paper, we take balance equally between the wavelength and the location as $\rho_i = 1$.

Experiments

The feasibility of the proposed method was examined in details using pairs of fluorescent object samples. The light sources used in the experiments were an incandescent lamp and an artificial sunlight lamp (SERIC XC-100). The spectral imaging system consisted of a monochrome CCD camera (QImaging Retiga 1300), a VariSpec LCT filter, and a personal computer. The spectral images were captured at an equal wavelength interval of 5 nm in the visible range (400, 700 nm). Therefore, each captured image was represented in an array of 61-dimensional vectors. The Donaldson matrix of a fluorescent object was estimated by the two illuminant projection method [12] using the incandescent lamp and the sunlight lamp. In experiments, we placed two fluorescent boards at an angle of 90 degrees on a table covered with a black cloth. The sizes of the boards were 10cm by 10cm. When the light source was straight in front of the object, interreflection effect was observed around the boundary between the two surfaces.

Figures 3 (a) and (b) show the observed images of a yellow fluorescent board (left) and a red fluorescent board (right) under the two light sources. The image size is 413 × 557 pixels. We see clearly color changes in the intersection regions as the results of the strong interreflection effects. Note that the object color at the right side reflects on the left surface. We cut a 60 pixel width image across the intersection out of the most influenced region of the original images. Figures 3 (c) and (d) show the observed images in the narrow regions. Although the Donaldson matrices for the two surfaces were obtained at these regions, the spectral functions were distorted from the original features.

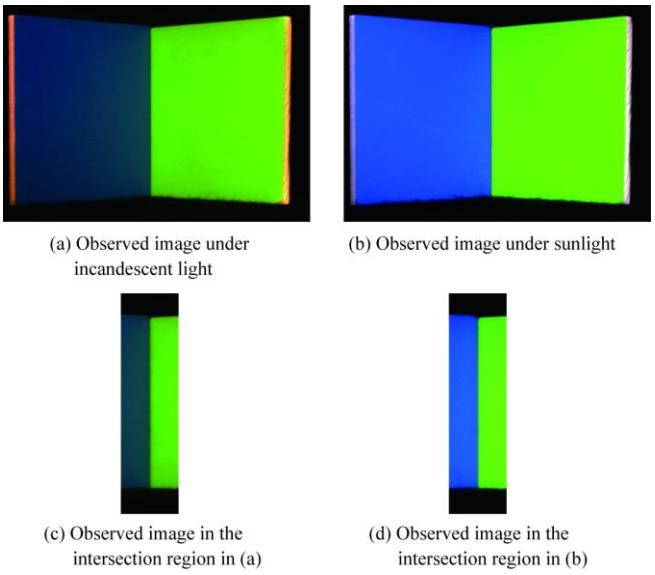

Figure 3. Observed images and cut images. (a) and (b): observed images of a blue fluorescent board (left) and a green fluorescent board (right) under the two light sources. (c) and (d): cut images with narrow width around the intersection out of the original image.

Under the condition that the Donaldson matrix is unknown, we adopted the two step estimation procedure to define the most appropriate estimates of the spectral functions. First, the iterative estimation algorithm was used to find the best estimates under the norm constraint. The solid lines in Figure 4 represent the initial spectra in the iterative algorithm, where we assumed $\|\mathbf{s}_1\| = \|\mathbf{s}_2\| = 2.5$, $\|\boldsymbol{\alpha}_1\| = \|\boldsymbol{\alpha}_2\| = 0.5$. Second, the norms of the spectral functions were adjusted based on the smoothness index for the spectral functions and the location weights. Figure 5 shows the estimation results of the spectral functions. The broken curves (Estimate 1) in Figure 5 represent the estimates after five iterations of the iterative estimation algorithm. Large errors remain in the reflectance and emission estimates of $\hat{S}_1(\lambda)$ and $\alpha_2(\lambda)$. The bold curves (Estimate 2) in Figure 5 represent the final estimates after the second step.

The scale factors of adjusting the norms were determined as K_1 = 0.76, K_2 = 0.96, K_3 =1.04, and K_4 = 0.83 after roughness computation of the spectral functions and the location weights in Eq.(11). The estimation accuracy for the diffuse reflectance $\hat{S}_1(\lambda)$ was greatly improved. Figure 6 represents the estimation results for the excitation spectra, which were determined using the reflectance estimates in Eq. (9).

Figure 7 shows the estimated location weights for the respective components. Figure 8 demonstrate the component images (a)-(c) and the constructed images (d) of the two surfaces under the incandescent light and the sunlight. It should be noted that relighting the two surfaces under arbitrary illuminant and displaying the component images can be performed by using the estimated spectral functions and the estimated location weights.

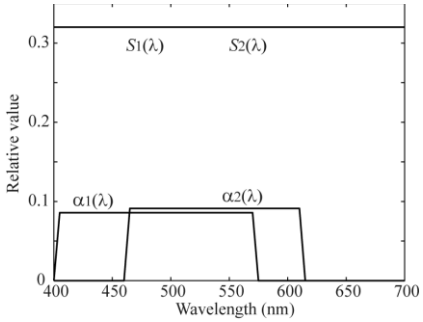

Figure 4. Constant spectra as initial conditions of the iterative algorithm.

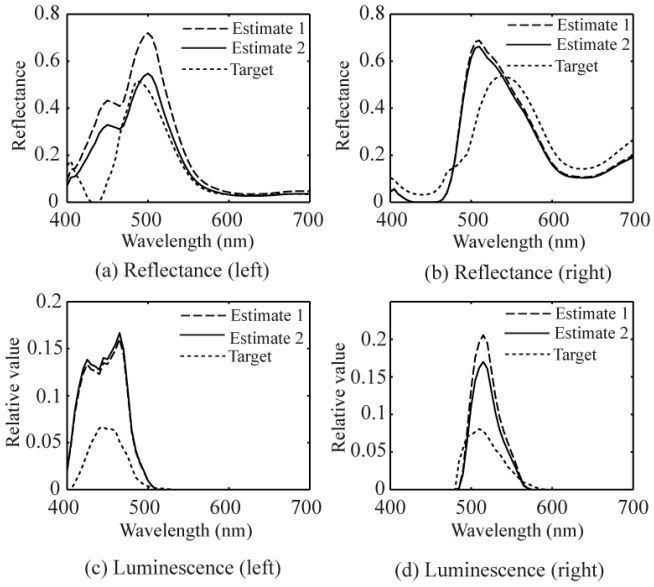

Figure 5. Estimation results of the spectral functions in the two steps, where Estimate 1 represents the estimates by the iterative estimation algorithm and Estimate 2 represents the final estimates after the scale adjustment of the norms.

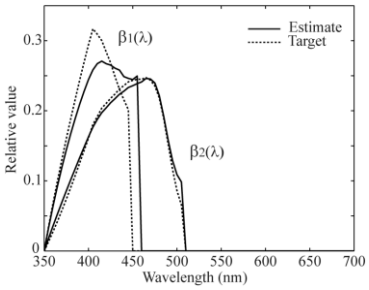

Figure 6. Estimation results for the excitation spectra of the blue-green objects.

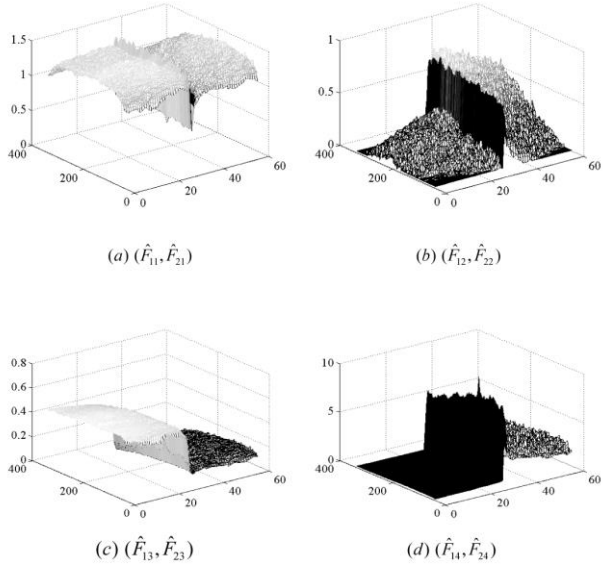

Figure 7. Estimated location weights for the respective components of the observed images in Figures 3 (c) and (d).

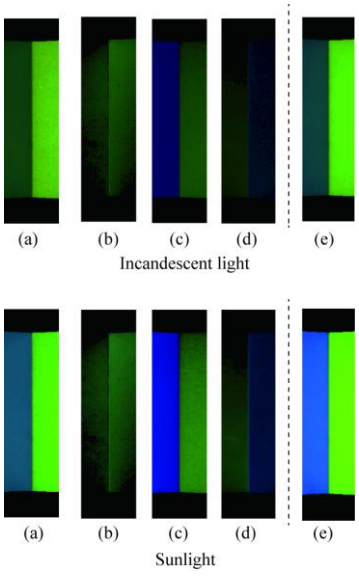

Figure 8. Component images (a)-(d) of the observations under two light sources and reconstructed images (e) from (a)-(d).

Conclusions

The present paper has proposed a method to analyze the observed images of fluorescent images influenced by mutual illumination and estimate the spectral components. The observed image of mutual illumination was modeled by sum of products of the spectral component functions and their location weights on the surfaces. We showed that the spectral composition was summarized with four components. In order to solve the nonlinear estimation problem, we developed an iterative algorithm to estimate the spectral functions and the location weights. Moreover, in order to estimate the norms of the spectral functions, we adopted a stabilization index to enforce the spectral smoothness and the spatial smoothness. An advantage of the present algorithm is that the Donaldson matrix is not necessary as the initial condition. In experiments, the feasibility was shown for two adjacent fluorescent objects with mutual illumination effects. The present model and estimation method can be applied to general objects with matte surfaces without glosses or highlights. The norm estimation of spectral functions is not applicable to uneven object surfaces.

Acknowledgment

This work was supported by JSPS KAKENHI Grant Number JP15H05926 (Grant-in-Aid for Scientific Research on Innovative Areas “Innovative SHITSUKSAN Science and Technology”).

References

[1] J. J. Koenderink and A. J. van Doorn, Geometrical modes as a general method to treat diffuse interreflections in radiometry, J. Optical Society of America, Vol. 73, No. 6, pp. 843-850, 1983.

[2] D. Forsyth and A. Zisserman, Mutual illumination, Proceedings of 1989 Computer Vision and Pattern Recognition (CVPR '89), pp. 466-473, 1989.

[3] S.K. Nayar, K. Ikeuchi, and T. Kanade, Shape from Interreflections, Int. J. Computer Vision, Vol.6, No.3, pp.173-195, 1991.

[4] M.S. Drew and B.V. Funt, Variational approach to interreflection in color images, J. Optical Society of America A, Vol. 9, No. 8, pp.1255-1265, 1992.

[5] R. Bajcsy, S.W. Lee, and A. Leonards, Detection of diffuse and specular interface reflections and inter-reflections by color image segmentation, Int. J. Computer Vision, Vol. 17, No.3, pp. 241-272, 1996.

[6] S. Tominaga, Separation of reflection components from a color image, Proceedings IS&T/SID’s 19th Color Imaging Conference (CIC5), pp. 254-257, 1997.

[7] M. Langer, Model of how interreflections can affect color appearance, Color research and application, Supplement Vol. 26, pp. S218-S221, 2001.

[8] S.K. Nayar, G. Krishnan, M.D. Grossberg, and R. Raskar, Fast separation of direct and global components of a scene using high frequency illumination, ACM SIGGRAPH, pp. 935–944, 2006.

[9] S. Tominaga, K. Kato, K. Hirai, and T. Horiuchi, Bispectral interreflection estimation of fluorescent objects, Proceedings 23th Color and Imaging Conference (CIC23), 2015.

[10] S. Tominaga, K. Kato, K. Hirai, and T. Horiuchi, Spectral image analysis of mutual illumination between florescent objects, J. Optical Society of America A, Vol. 33, No. 8, pp.1476-1487, 2016.

[11] R. Donaldson, Spectrophotometry of fluorescent pigments, British J. of Applied Physics, Vol.5, pp.210-214, 1954.

[12] S. Tominaga, K. Hirai, and T. Horiuchi, Estimation of bispectral Donaldson matrices of fluorescent objects by using two illuminant projections, J. Optical Society of America A, Vol. 32, No. 6, pp.1068-1078, 2015.

Author Biography

Shoji Tominaga received the B.E., M.S., and Ph.D. degrees in electrical engineering from Osaka University, Osaka, Japan, in 1970, 1972, and 1975, respectively. In 2006, he joined Chiba University, Japan, where he was a Professor (2006-2013) and Dean (2011-2013) at Graduate School of Advanced Integration Science. He is now a Specially Appointed Researcher, Chiba University. His research interests include digital color imaging, multispectral image analysis, and material appearance modeling. He is a Fellow of IEEE, IS&T, and SPIE.